Dalton Transactions

PAPER

View Article Online
View Journal | View Issue

Cite this: *Dalton Trans.*, 2017, **46**, 15407

Facile generation of iridium $PC_{carbene}P$ pincer complexes *via* water elimination from an alcohol proligand†

Simon Sung and Rowan D. Young *

We report the facile generation of Ir $PC_{carbene}P$ pincer systems. These systems are accessed from the reaction between $[IrCl(COD)]_2$ and a bis(diphenyl)phenylene P(OH)P proligand (**1**) with concomitant dehydration, followed by salt metathesis/ligand exchange in the case of cationic examples. In contrast to previously reported double C–H activation synthetic strategies to access similar complexes, accessing Ir $PC_{carbene}P$ complexes through dehydration proceeds rapidly at room temperature and provides the first example of the incorporation of phosphino aryl substituents. The generated complexes are shown to possess the ability to activate inert C–H bonds and partake in ligand cooperativity. Mechanistic evidence suggests that divergent C–H and O–H activation pathways of ligand **1** ultimately lead to the same Ir $PC_{carbene}P$ product (**2**). It is hoped that the stability and synthetic accessibility of these complexes will encourage their increased use in catalyst surveys.

Received 1st October 2017,
Accepted 23rd October 2017

DOI: 10.1039/c7dt03690f

rsc.li/dalton

Introduction

Pincer ligands are tridentate *meridional* ligands that offer unique rigidity, selective activity and complex stability for transition metal centers.[1] Such ligands have played an instrumental role in the development of transition metal catalysts capable of performing difficult bond transformations. Among various pincer ligand scaffolds, PCP type pincers, containing a metal–carbon bond, enable the exploits of organometallic chemistry to be invoked for a range of bond transformations and/or catalysis. PCP pincers can be classified based on the hybridization of the metal bound carbon donor, namely as either sp^3 or sp^2 (sp PCP pincers are yet to be reported).

The sp^2 PCP pincer ligand class is dominated by aromatic based designs, where the central carbon donor belongs to an aromatic system. However, $PC_{carbene}P$ pincers, where the central carbon is an alkylidene donor, have displayed unique reactivity due to their extremely strong *trans* effect and their ability to partake in ligand–metal cooperativity.[2,3]

$PC_{carbene}P$ pincers have been readily accessible for Ir, Ru and Os centres since early reports by Shaw, and then Gusev demonstrated double C–H activation.[4] However, the alkyl backbones of such systems were unstable and conducive to β-hydride elimination. More recently, Ozerov (and later Piers) introduced β-hydride elimination resistant $PC_{carbene}P$ ligands.[5] Since then, the metals accommodated in $PC_{carbene}P$ scaffolds have expanded to include Ni, Pd and Rh.[2a,g,6] However, accessing $PC_{carbene}P$ pincers through double C–H activation is limited to noble metals well-known for their C–H activation abilities (Ni $PC_{carbene}P$ complexes were accessed through HX elimination). Perhaps because of this, much attention has been focused on various designs of iridium $PC_{carbene}P$ pincer complexes (Fig. 1).

Reports have demonstrated the ability of iridium $PC_{carbene}P$ pincer complexes to reversibly activate E–H bonds (E = H, O, N, C), perform challenging catalysis, and to partake in difficult redox and catalytic processes.[7] The exploration of iridium $PC_{carbene}P$ pincer complexes has led to a variety of pincer designs incorporating various carbocycles and heterocycles into the spinal positions, and featuring a range of phosphino alkyl substituents. However, phosphino donors with aryl substituents are yet to be reported, despite their higher stability, affordability and easier synthetic/commercial access as compared to alkyl phosphines. This is likely due to the need for electron rich metal centres to induce double C–H activation. As such, the powerful reactivity presented by iridium $PC_{carbene}P$ pincer complexes has only been utilized by synthetic organometallic groups capable of synthesizing and handling alkyl phosphino $PC_{carbene}P$ pincer proligands.

We have recently reported the protonolysis of rhodium α-hydroxyalkyl complexes to access $PC_{carbene}P$ pincer complexes, avoiding double C–H activation.[8] Herein, the formal de-

Department of Chemistry, National University of Singapore, 3 Science Drive 3, Singapore 117543. E-mail: rowan.young@nus.edu.sg

† Electronic supplementary information (ESI) available. CCDC 1568119–1568125. For ESI and crystallographic data in CIF or other electronic format see DOI: 10.1039/c7dt03690f

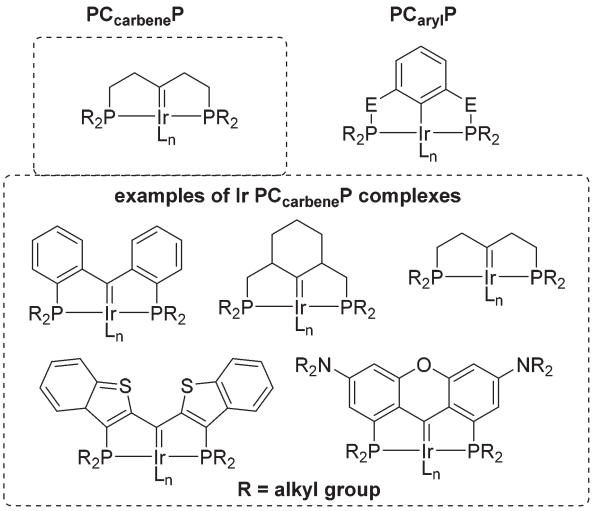

Fig. 1 (Above) Ir sp^2 PCP architectures based on alkylidenyl and aryl carbon attachments. (Below) Examples of selected PC$_{carbene}$P architectures.

hydration of an air-stable bis(diphenylphosphino) alcohol POP pro-ligand to an iridium PC$_{carbene}$P pincer complex is detailed. Competing C–H and O–H activation is suggested with the isolation of a rare α-hydroxylalkyl complex and an iridium alkoxide intermediate. Although other PC$_{carbene}$P iridium complexes featuring diaryl phosphino substituents have yet to be reported in the literature, the activity of the iridium PC$_{carbene}$P^{Ph} platform is demonstrated with ligand exchange and C–H activation chemistry under mild conditions.

Results and discussion

Addition of compound **1** to [IrCl(COD)]$_2$ results in rapid generation of the PC$_{carbene}$P complex **2** and liberation of H_2O and 1,5-cyclooctadiene (COD) (Scheme 1). At room temperature, ^{31}P NMR suggested that conversion to **2** was >50% after 15 minutes. In comparison, double C–H activation approaches to generate Ir PC$_{carbene}$P^{alkyl} complexes require prolonged heating (hours) above 100 °C.[5b] Compound **2** was isolated in high yield (76%) *via* precipitation with *n*-hexane.

Compound **2** possesses a single ^{31}P NMR resonance at δ_P 29.0, and a ^{1}H NMR spectrum of **2** displays only aryl proton resonances, which provide little definitive evidence for the identity of **2**. However, ^{13}C NMR spectroscopic data for **2** revealed a highly deshielded triplet signal at 207.4 ppm ($^2J_{CP}$ = 2.8 Hz), supporting the assigned alkylidene attachment. X-ray quality crystals of **2**, grown by vapour diffusion between *n*-hexane and a concentrated solution of **2** in DCM at room temperature, allowed a diffraction study to be performed. From this, the determined molecular structure of **2** (Fig. 2) confirmed the formation of the PC$_{carbene}$P backbone, with an Ir1–C1 bond length of 1.940(2) Å suggestive of Ir–C double bond character (*cf.* 1.899(7) Å for the PC$_{carbene}$P^{iPr} analogue).[5b] This Ir=C bond length lies within the range of previously reported iridium PC$_{carbene}$P complexes, with a minimum observed value of 1.86(1) Å and a maximum value of 2.038(9) Å.[6b,7c]

The molecular structure of **2** reveals that **2** possesses C_2 symmetry, as opposed to C_{2v} symmetry, as often observed in aryl PCP pincer complexes. Consequently, **2** exists as a racemic mixture of *R* and *S* conformers.

Cationic iridium PC$_{carbene}$P complexes could be generated *via* salt metathesis between Na[BAr$^F_4$] and compound **2** in the presence of a suitable ligand. Such methodology has been previously described by Piers.[6b,9] Thus, compounds **3** and **4** were generated by the addition of Na[BAr$^F_4$] to an equimolar amount of **2** and either PPh_3 or PCy_3 respectively (Scheme 1). The molecular structures of **3** (Fig. 3) and **4** (Fig. 4) reveal slightly elongated Ir1–C1 distances in the cationic complexes {1.994(8) Å in **3** and 1.953(8) Å in **4**}, reflecting the sensitivity of the π-acidic alkylidene linkage to electron density change at the iridium centre due to the π-basic nature of the chloride ligand in **2** and the cationic nature of complexes **3** and **4**.

The ^{13}C NMR resonances arising from the carbenic carbon positions in compounds **2**, **3** and **4** follow the trend that **2** (δ_c 207.4) < **4** (δ_c 231.9) < **3** (δ_c 241.6). This trend roughly correlates with Ir=C bond lengths, and reflects an increase in 'free' carbene character from **2** to **4** to **3**.[10]

Metathesis of **2** in the presence of two equivalents of PPh_3 led to the formation of metallacycle **5** (Fig. 5). Compound **5**

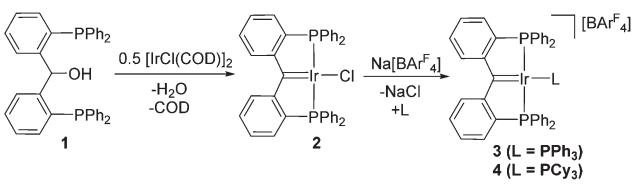

Scheme 1 Synthesis of PC$_{carbene}$P iridium complex **2** *via* dehydration of ligand **1**. Metathesis of **2** with Na[BAr$^F_4$] in the presence of PPh_3 or PCy_3 generates **3** and **4** respectively.

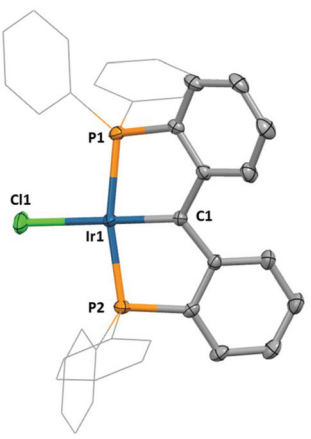

Fig. 2 Molecular structure of **2**. Hydrogen atoms omitted, thermal ellipsoids shown at 50%. Selected bond distances (Å) and angles (°): Ir1–P1, 2.291(1); Ir1–C1, 1.940(2); Ir1–Cl1, 2.350(3); C1–Ir1–Cl1, 180.0(1); P1–Ir1–P2, 166.0(1).

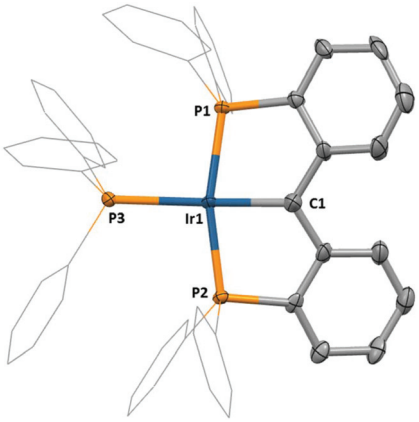

Fig. 3 Molecular structure of **3**. Hydrogen atoms and anion omitted, thermal ellipsoids shown at 50%. Selected bond distances (Å) and angles (°): Ir1–P1, 2.298(2); Ir1–C1, 1.994(8); Ir1–P2, 2.282(2); Ir1–P3, 2.394(2); C1–Ir1–P3, 178.3(3); P1–Ir1–P2, 164.1(1).

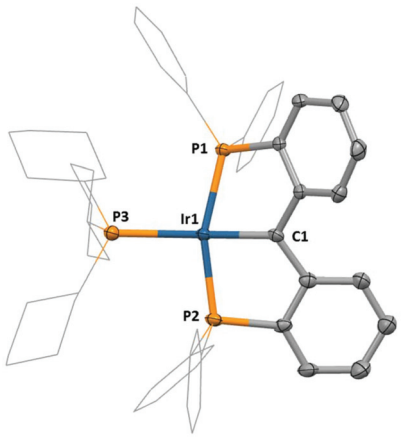

Fig. 4 Molecular structure of **4**. Hydrogen atoms and anion omitted, thermal ellipsoids shown at 50%. Selected bond distances (Å) and angles (°): Ir1–P1, 2.269(2); Ir1–C1, 1.953(8); Ir1–P2, 2.317(2); Ir1–P3, 2.423(2); C1–Ir1–P3, 169.2(2); P1–Ir1–P2, 158.0(1).

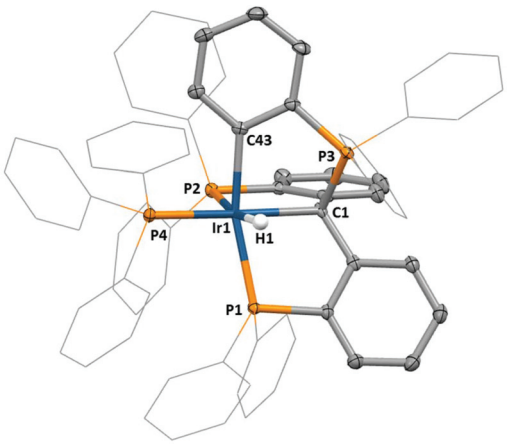

Fig. 5 Molecular structure of **5**. Hydrogen atoms (except H1) and anion omitted, thermal ellipsoids shown at 50%. H1 was located in a Fourier Difference map. Selected bond distances (Å) and angles (°): Ir1–P1, 2.343 (1); Ir1–C1, 2.232(3); Ir1–P2, 2.397(1); Ir1–P4, 2.343(1); Ir1–C43, 2.095(3); C1–P3, 1.840(4); C1–Ir1–P4, 172.5(1); P1–Ir1–C43, 162.53(9).

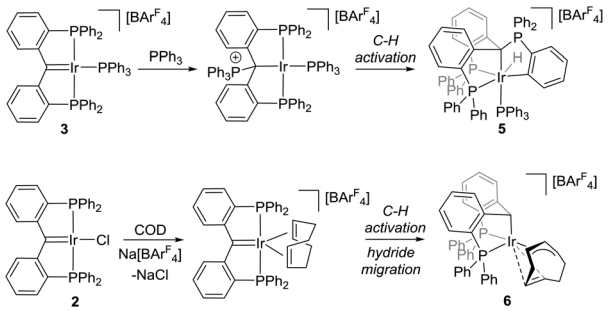

Scheme 2 (Above) Reaction of **3** with PPh_3 results in ligand cooperative C–H activation of PPh_3. (Below) A cationic $PC_{carbene}P$ intermediate, generated *via* metathesis of Na[BAr^F_4] with **2**, C–H activates 1,5-cyclooctodiene generating iridium(III) allyl **6**.

could also be generated by adding an equivalent of PPh_3 to isolated **3** (Scheme 2). Thus, **5** is likely generated *via* coordination of PPh_3 to the electrophilic carbene position in **3** and subsequent cyclometallation at the iridium centre. Cyclometallation of PPh_3 is well-documented on iridium,[11] but iridium-alkylidene cooperative cyclometallation is less reported.[12] Such a ligand directed substrate activation mirrors cooperative PPh_3 C–H activation and CO_2 activation on related ruthenium vinylidene and carbodiphosphorane complexes.[13]

We recently reported the rhodium analogue of **3**, [$PC_{carbene}P^{Ph}Rh(PPh_3)$][$BAr^F_4$].[8a] Although the rhodium carbene position was found to be electrophilic in this complex, it was stable in the presence of excess PPh_3, even upon heating. By comparison, the carbene position in **3** proves to be much more electrophilic than its rhodium analogue. This is somewhat expected, given that iridium stablises the singlet state of the carbene ligand to a greater extend than rhodium.

Metathesis of **2** in the presence of 1,5-cyclooctadiene as the supporting ligand led to product **6** (Scheme 2). A molecular structure of compound **6** (Fig. 6) reveals that the COD ligand had undergone C–H activation, resulting in an allylic coordination. The concomitantly generated hydrido group then transfers from the iridium centre to the carbene ligand transforming the pincer into a *facially* coordinated $PC_{sp^3}P$ ligand, which is also evident by ^{1}H NMR analysis that reveals a resonance at 4.59 ppm correlating to this hydrogen. The resulting Ir–C bond distance in the $PC_{sp^3}P$ ligand of **6** is observed at a increased length of 2.158(4) Å (*cf.* 1.890(4) Å in **2**).

The activation of C–H bonds, and also C–C bonds, in iridium dienes is well known in accessing resonance stabilised ligands.[14]

Compound **6** could also be generated directly by heating compound **1** and [$Ir(COD)_2$][BAr^F_4] at 95 °C for 18 hours. The stability of **6** supports the premise that electron poor iridium centres perform poorly at α-hydrogen elimination. In sharp contrast, cationic iridaepoxide complexes, or intermediates

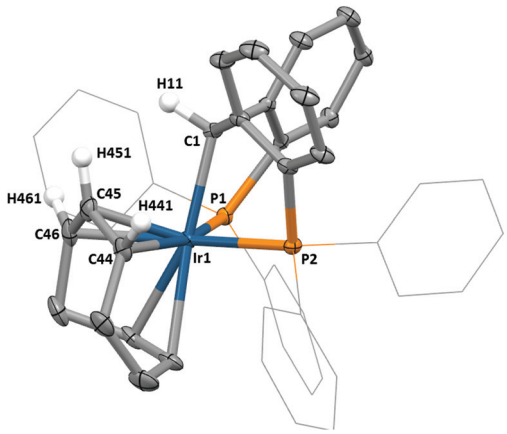

Fig. 6 Molecular structure of **6**. Hydrogen atoms (except H11, H441, H451 and H461) and anion omitted, thermal ellipsoids shown at 50%. Selected bond distances (Å) and angles (°): Ir1–P1, 2.298(1); Ir1–C1, 2.158(4); Ir1–P2, 2.328(1); C44–C45, 1.422(7); C45–C46, 1.420(7); C1–Ir1–P1, 80.7(1); P1–Ir1–P2, 102.2(1).

en route to **2** (see below) readily undergo α-hydroxyl elimination, suggesting that this may be a more facile process.[9]

It was found that the presence of PPh_3 arrested the reaction between **1** and $[IrCl(COD)]_2$, and prevented formation of **2**. As such, treatment of compound **1** with $[IrCl(COD)PPh_3]$ at room temperature followed by heating at 55 °C for 2 days led to a mixture of two products, alkoxide **7a** and α-hydroxylalkyl **7b** in a 1 : 4 ratio according to the relative integrations by ^{31}P NMR spectroscopy (Scheme 3). Fractional crystallization allowed the isolation and characterization of each compound.

The structure of **7a** was established *via* ^{1}H, ^{13}C and ^{31}P NMR spectroscopies. Correlation spectroscopy confirmed the formulation of **7a** as an alkoxide, with a ^{13}C NMR resonance at δ_c 78.7 correlating strongly to a methine proton at δ_H 5.05 in a HSQC experiment (see ESI†). Strong ^{31}P coupling observed for the signal at δ_H 5.05 suggested a *trans* PPh_3 position. The *mer* configuration of the pincer was established by ^{31}P NMR, where two signals were observed in a 2 : 1 ratio at δ_P −6.1 (2 P, d, $^{2}J_{PP}$ = 11.4 Hz) and −1.2 (1 P, t, $^{2}J_{PP}$ = 11.4 Hz).

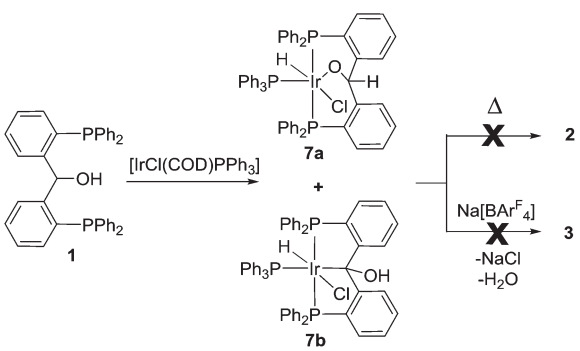

Scheme 3 PPh_3 arrests the dehydration of **1**, with formation of **7a** and **7b** (1 : 4 ratio). Heating **7a** or **7b** failed to generate **2**, and reaction with $Na[BAr^{F}_4]$ failed to generate **3**.

Compound **7b** represents a direct route to access an iridium α-hydroxylalkyl, with previous reported examples either relying on formation of the α-hydroxyalkyl moiety within the metal coordination sphere, or being resonance supported forms better described as protonated β-diketones.[15] X-ray diffraction quality crystals of **7b** allowed the determination of its molecular structure (Fig. 7). The structure of **7b** reveals that it is coordinatively saturated (O_h geometry), preventing potential α-hydroxyl elimination.

In order to investigate which of **7a** or **7b** represents a more likely model intermediate for the formation of **2**, samples of each were heated to promote PPh_3 dissociation. However in both cases, our inability to eliminate coordinated PPh_3 prevented transformation of **7a** or **7b** into **2**.

Addition of $Na[BAr^{F}_4]$ to either complexes **7a** or **7b** readily led to metathesis, but failed to generate a cationic iridium $PC_{carbene}P$ complex (*i.e.* **3**) even when heated to 80 °C. This is in contrast to previously described rhodium analogues, and may suggest against a proton transfer mechanism for dehydration. In the case of **7a**, the known cation fragment $[Ir(CO)(PPh_3)_3][BAr^{F}_4]$[16] was generated as the sole product, whereas **7b** decomposed into multiple unknown products. Piers has reported the decomposition of $[\kappa^3\text{-}P'(\eta^2\text{-}CO)P''IrCl]$ iridaepoxides into related $[IrCl(CO)(PR_3)_2]$ products, suggesting a plausible decomposition route that proceeds *via* the β-hydride elimination in **7a**.[17]

Monitoring of the reaction between **1** and $[IrCl(COD)]_2$ at various temperatures between 253 K and 298 K revealed that intermediate complex **I** forms prior to any bond activation (Scheme 4). The ^{1}H NMR spectrum of complex **I** at 263 K displays a downfield signal at 11.07 ppm that has been associated with a C–H/metal anagostic interaction in related rhodium intermediates.[6a,8a] However, ^{1}H–^{13}C NMR correlation experiments, and isotopic labelling experiments suggested the signal was due to the OH motif (see ESI†). Thus, the interaction

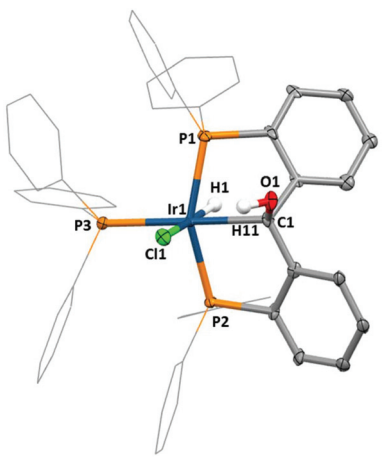

Fig. 7 Molecular structure of **7b**. Hydrogen atoms (except H1 and H11) omitted, thermal ellipsoids shown at 50%. H1 and H11 were located in a Fourier Difference map. Selected bond distances (Å) and angles (°): Ir1–P1, 2.296(2); Ir1–C1, 2.195(9); Ir1–P2, 2.310(2); Ir1–P3, 2.369(3); Ir1–Cl1, 2.499(2); C1–Ir1–P3, 175.6(3); P1–Ir1–P2, 154.0(1).

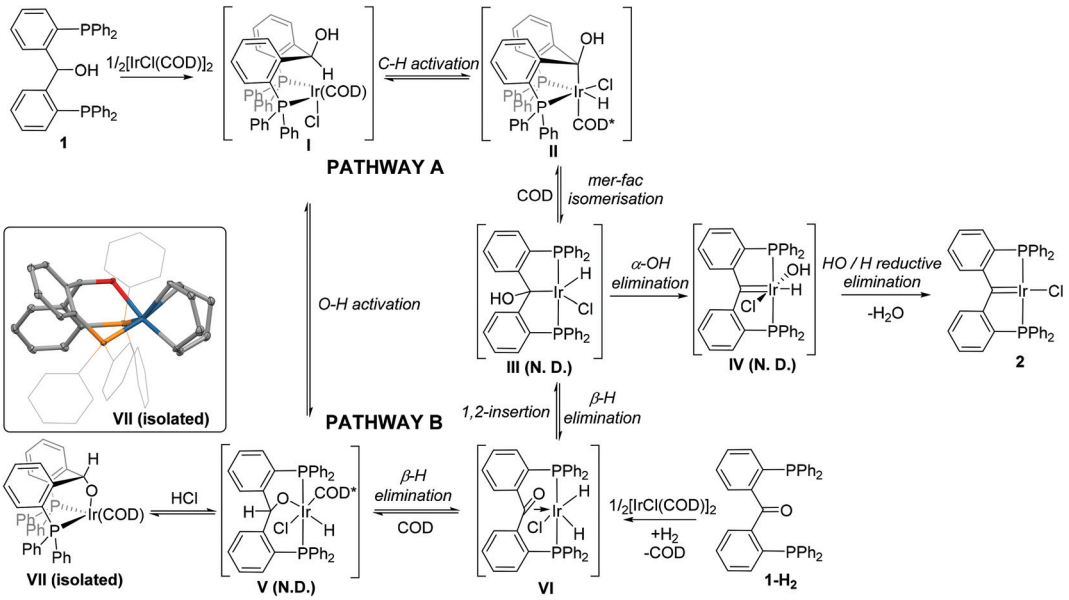

Scheme 4 Possible reaction mechanism for the formation of **2**. * denotes κ^1-COD coordination. N. D. denotes not detected by NMR spectroscopy.

between the linkage of ligand **1** and the metal centre in complex **I** can not be defined with any certainty.

Given that compound **1** has been shown to be susceptible to O–H and C–H activation (*i.e.* in generation of **7a–b**), it is possible that both intermediates **II** and **VI** shown in Scheme 4 could be produced upon C–H or O–H activation (respectively) of the chelate ligand in **I**, representing divergent reaction pathways.

At 253 K, as complex **I** diminishes in concentration, two independent iridium hydride species are observed, complexes **II** and **VI**. Intermediate **II** was characterized by ^{1}H and ^{31}P NMR spectroscopy, and by reaction with isotopologues **1a** and **1b** that contained deuterated methine and hydroxyl positions respectively (see ESI†). Intermediate **II** supports a C–H activation pathway (pathway A, Scheme 4) that proceeds *via* an α-hydroxylalkyl complex. In contrast to **7b**, complex **II** is characterized by a *fac* coordination of the α-hydroxyalkyl ligand. The flexibility of $PC_{sp^3}P$ ligands, related to **1**, to adopt both *fac* and *mer* configurations is well-documented.[18] As the signal intensities from **II** diminish, signals for product **2** grow in intensity.

Isomerisation of the tridentate PCP ligand from *fac* to *mer* generates **III**. Concomitant dissociation of COD would allow this process to proceed *via* a 5-coordinate intermediate, as has been reported for related Rh(III) POP pincer systems.[19]

As stated above, addition of $Na[BAr^F_4]$ to either complexes **7a** or **7b** failed to generate a cationic iridium $PC_{carbene}P$ complex (*i.e.* **3**). This may imply that formation of **2** proceeds *via* α-hydroxyl elimination in **III** to give **IV**, as suggested by Piers,[2b,c,9] rather than proton transfer from iridium to the α-hydroxylalkyl position to give **V**, which was observed for more Brønsted acidic rhodium examples.[8a] α-Alkyl elimination in closely related iridium PCP complexes has been directly observed by Wendt.[20] The product of C–O activation, intermediate **IV** (Scheme 4), can then undergo H/OH reductive elimination to give **2** and eliminate water.

The hydrido complex **VI** was observed simultaneously with **II**, and represents the β-hydrogen elimination product of an initial O–H activation intermediate (**V**) for pathway B (Scheme 4). Intermediate **VI** was characterized by ^{1}H, ^{31}P NMR spectroscopy, and reaction with isotopologues **1a** and **1b**. Although the hydride positions in **VI** are inequivalent, dynamic exchange between the positions gives rise to a single triplet signal at δ_H −12.57. The possibility of **VI** existing as a dihydrogen complex was precluded by the absence of any observable D–H coupling while employing isotopologues **1a–b**. Furthermore, **VI** displays an η^2-carbonyl ^{13}C NMR signal at δ_C 132.1, more indicative of an iridium(III) oxidation state.[2c]

Intermediate **VI** can in-principle also be generated from β-hydride elimination from an α-hydroxylalkyl ligand (*i.e.* from **III** of pathway A, Scheme 4). Indeed, this likely marks the convergence of pathways A and B. However, using the isotopologue **1a** (methine position deuterated), very little of complex **II** is generated, and much higher concentrations of **VI** are observed, indicative of a notable kinetic isotope effect for C–H activation. From this reaction solution, X-ray quality crystals of complex **VII** precipitated. Structural characterization of **VII** demonstrates it to be an O–H activation product arising from HCl elimination from **V** (Scheme 4 inset). Indeed, addition of ethereal HCl to crystals of **VII** generated product **2** and intermediates **I**, **II** and **VI**, which indicates the presence of equilibria between species of pathways A and B.

Further evidence for the identity of **VI** is garnered from the addition of the dehydrogenated, keto form of **1** (**1-H$_2$**), with $[IrCl(COD)]_2$ under a H_2 atmosphere. At room temperature, intermediates **VI** and **VII** are readily identified as the major species after 5–10 minutes, after which time **2** is generated. However, this does not represent a practical synthesis of **2**, as

it was found that **2** further reacts with H_2 to give hydrogenation products.

Conclusions

In conclusion, we have reported a facile method of accessing iridium $PC_{carbene}P$ complexes *via* dehydration of an alcoholic bisphosphino proligand. Mechanistic studies suggest two competing, divergent C–H and O–H activation pathways, ultimately leading to the same iridium $PC_{carbene}P$ product (**2**). The above described reactivity demonstrates the activity of the $PC_{carbene}P^{Ph}$ platform. This system is able to partake in ligand–metal cooperativity to perform difficult bond activations such as C–H activation, as demonstrated in the generation of compounds **5** and **6**. Given recent reports of the use of $PC_{carbene}P$ iridium complexes in catalysis, the ability to access this ligand platform from stable, commercially available (or simple to synthesise and store) components allows synthetic chemists a potentially new catalytic tool for difficult transformations that have already been demonstrated in-practice using previously reported $PC_{carbene}P$ complexes.

Experimental

See ESI† for general experimental conditions.

Preparation of complex 2

A solution of $[IrCl(COD)]_2$ (134.3 mg, 0.20 mmol) in DCM (3 mL) was treated with a solution of compound **1** (221.0 mg, 0.40 mmol) in DCM (3 mL) at room temperature to give a green coloured solution and then stirred at room temperature for 30 h in a closed vessel. The solution was filtered and then the filtrate was evaporated. The residue was washed with *n*-hexane (3 × 10 mL) and then dissolved in DCM (3 mL), layered with *n*-hexane (5 mL) and left to stand at room temperature. The resultant green solid of complex **2** were isolated by filtration and then dried under vacuum (231 mg, 76%).

^{1}H NMR (500 MHz, CD_2Cl_2, 298 K) δ_H 6.85 (2 H, t, J = 7.4 Hz, Ar–H), 7.34–7.41 (2 H, m, Ar–H), 7.41–7.57 (12 H, m, PPh_2 H′s), 7.77–8.02 (8 H, m, PPh_2 H′s), 8.20 (2 H, d, J = 7.6 Hz, Ar–H), 8.26–8.31 (2 H, m, Ar–H). $^{13}C\{^1H\}$ NMR (126 MHz, CD_2Cl_2, 298 K) δ_C 124.6 (t, J = 7.3 Hz), 129.1 (t, J = 5.2 Hz), 129.2 (s), 131.0 (s), 132.1 (t, J = 25.0 Hz), 133.8 (s), 134.6 (t, J = 6.9 Hz), 137.0 (s), 138.5 (t, J = 24.1 Hz), 174.8 (t, J = 19.2 Hz), 207.4 (t, $^2J_{CP}$ = 2.8 Hz, Ir=C). $^{31}P\{^1H\}$ NMR (202 MHz, CD_2Cl_2, 298 K) δ_P 29.0 (2 P, s, PCP pincer P′s). HRMS (ESI-TOF) *m*/*z*: $[M + H]^+$ calcd for $C_{37}H_{29}ClIrP_2$ 763.1050; found 763.1021. Elemental analysis: calc. for $C_{37}H_{28}ClIrP_2$: C, 58.3; H, 3.7; found: C, 58.1; H, 3.7%.

Preparation of complex 3

A solution of complex **2** (22.9 mg, 0.030 mmol) in DCM (5 mL) at −78 °C was treated dropwise with a solution of $Na[BAr^F_4]\cdot 2THF$ (34.0 mg, 0.033 mmol) in DCM (5 mL) and then a solution of PPh_3 (7.9 mg, 0.030 mmol) in DCM (5 mL). The solution was allowed to slowly come to room temperature and was stirred for an additional 2 hours. The reaction mixture was filtered and then the filtrate was evaporated to approx. 1 mL. The solution was layered with *n*-hexane (10 mL) and then left to stand at room temperature. Dark green crystals of **3** were isolated by filtration and then dried under vacuum (38 mg, 68%).

^{1}H NMR (500 MHz, CD_2Cl_2, 298 K) δ_H 6.77 (6 H, ddd, J = 11.2 Hz, J = 8.2 Hz, J = 1.4 Hz, Ar–H), 6.97 (6 H, td, J = 7.9 Hz, J = 2.1 Hz, Ar–H), 7.05 (2 H, t, J = 7.6 Hz, Ar–H), 7.20–7.29 (10 H, m, Ar–H), 7.29–7.49 (15 H, m, Ar–H), 7.56 (4 H, s, $[BAr^F_4]$ Ar–H), 7.73 (8 H, s, $[BAr^F_4]$ Ar–H), 7.96 (2 H, d, J = 7.8 Hz, Ar–H), 8.35 (2 H, td, J = 7.5 Hz, J = 1.3 Hz, Ar–H). $^{13}C\{^1H\}$ NMR (126 MHz, CD_2Cl_2, 298 K) δ_C 117.7–118.1 (m, $[BAr^F_4]$ Ar–C), 121.5–128.3 (m), 128.6–129.0 (m), 129.2 (t, J = 5.2 Hz), 129.3–130.2 (m), 131.0 (d, J = 1.8 Hz), 131.7 (s), 133.3 (s), 133.6–133.8 (m), 134.3 (s), 134.6 (s), 134.6–134.9 (m), 135.2 (s, $[BAr^F_4]$ Ar–C), 135.5 (s), 145.3 (d, J = 7.1 Hz), 162.2 (q, $^1J_{CB}$ = 49.7 Hz, $[BAr^F_4]$ Ar–C), 169.3 (td, J = 18.7 Hz, J = 2.9 Hz), 241.6 (d, $^2J_{CP}$ = 72.7 Hz, Ir=C). $^{31}P\{^1H\}$ NMR (202 MHz, CD_2Cl_2, 298 K) δ_P 14.0 (1 P, t, $^2J_{PP}$ = 16.4 Hz, PPh_3), 30.8 (2 P, d, $^2J_{PP}$ = 16.4 Hz, PCP pincer P's). HRMS (ESI-TOF) *m*/*z*: $[M]^+$ calcd for $C_{55}H_{43}IrP_3$ 989.2206; found 989.2227. Elemental analysis: calc. for $C_{87}H_{55}BF_{24}IrP_3$: C, 56.4; H, 3.0; found: C, 56.0; H, 3.2%.

Preparation of complex 4

A solution of complex **2** (22.9 mg, 0.030 mmol) in DCM (5 mL) at −78 °C was treated dropwise with a solution of $Na[BAr^F_4]\cdot 2THF$ (34.0 mg, 0.033 mmol) in DCM (5 mL) and then a solution of PCy_3 (8.4 mg, 0.030 mmol) in DCM (5 mL). The solution was allowed to slowly come to room temperature and was stirred for an additional 2 hours. The reaction mixture was filtered and then the filtrate was evaporated to approx. 1 mL. The solution was layered with *n*-hexane (10 mL) and then left to stand at room temperature. Dark green crystals of **4** were isolated by filtration and then dried under vacuum (43 mg, 77%).

^{1}H NMR (500 MHz, CD_2Cl_2, 298 K) δ_H 0.63–0.74 (5 H, m, Cy–H), 0.87–0.95 (4 H, m, Cy–H), 1.03–1.15 (5 H, m, Cy–H), 1.27–1.52 (16 H, m, Cy–H), 1.74–1.94 (3 H, m, Cy–H), 6.93 (2 H, t, J = 7.4 Hz, 2 H, Ar–H), 7.36 (2 H, dt, J = 7.7, 4.0 Hz, Ar–H), 7.50–7.68 (16 H, m, Ar–H), 7.70–7.82 (10 H, m, Ar–H), 7.99 (8 H, q, J = 5.7 Hz, Ar–H), 8.31–8.43 (2 H, m, Ar–H). $^{13}C\{^1H\}$ NMR (126 MHz, CD_2Cl_2, 298 K) δ_C 26.1 (s, Cy–C), 27.2 (d, $^2J_{CP}$ = 10.2 Hz, Cy–C), 30.7 (s, Cy–C), 38.4 (d, $^1J_{CP}$ = 20.1 Hz), 117.8–118.0 (m, $[BAr^F_4]$ Ar–C), 121.7–128.4 (m), 128.8–129.8 (m), 131.2 (t, J = 25.5 Hz), 132.3 (s), 132.9 (t, J = 3.2 Hz), 134.4 (s), 134.9 (s), 135.3 (s, $[BAr^F_4]$ Ar–C), 135.6 (t, J = 6.0 Hz), 145.7 (td, J = 24.9, 6.3 Hz), 162.2 (q, $^1J_{CB}$ = 49.8 Hz, $[BAr^F_4]$ Ar–C), 170.3 (td, J = 18.5, 2.8 Hz), 231.9 (d, $^2J_{CP}$ = 69.5 Hz, Ir=C). $^{31}P\{^1H\}$ NMR (202 MHz, CD_2Cl_2, 298 K) δ_P 21.2 (1 P, t, $^2J_{PP}$ = 16.9 Hz, PCy_3), 26.7 (2 P, d, $^2J_{PP}$ = 16.9 Hz, PCP pincer P′s). HRMS (ESI-TOF) *m*/*z*: $[M]^+$ calcd for $C_{55}H_{61}IrP_3$ 1007.3620; found 1007.3620. Elemental analysis: calc. for $C_{87}H_{73}BF_{24}IrP_3$: C, 55.9; H, 3.9; found: C, 55.9; H, 3.4%.

Preparation of complex 5

Method A: A solution of complex **2** (22.9 mg, 0.030 mmol) in DCM (5 mL) at −78 °C was treated dropwise with a solution of $Na[BAr^F_4]\cdot 2THF$ (34.0 mg, 0.033 mmol) in DCM (5 mL) and then a solution of PPh_3 (19.7 mg, 0.075 mmol) in DCM (10 mL). The solution was allowed to slowly come to room temperature and was stirred for an additional 2 hours. The reaction mixture was filtered and then the filtrate was evaporated fully. *n*-Hexane was added to the residue, triturated and then decanted. This process was repeated two additional times. The remaining residue was dissolved in DCM (1 mL), layered with *n*-hexane (10 mL) and then left to stand at room temperature. Light yellow crystals of **5** formed from the solution were isolated by filtration and then dried under vacuum (45 mg, 71%).

Method B: PPh_3 (1.4 mg, 5.5 μmol) was added to a solution of complex **3** (9.3 mg, 5 μmol) in CD_2Cl_2 (0.6 mL) at room temperature. The reaction solution was mixed well and then left to stand at room temperature overnight. ^1H and ^{31}P NMR analyses confirmed the formation of complex **5** in quantitative yield.

^1H NMR (500 MHz, CD_2Cl_2, 298 K) δ_H −9.63 (1 H, dddd, J_{HP} = 133.1, 20.6, 17.0, 7.6 Hz, Ir–H), 5.985–6.09 (4 H, m, Ar–H), 6.23–6.33 (1 H, m, Ar–H), 6.46 (1 H, t, J = 8.2 Hz, Ar–H), 6.59–6.72 (3 H, m, Ar–H), 6.79–7.22 (37 H, m, Ar–H), 7.24–7.42 (4 H, m, Ar–H), 7.44–7.65 (8 H, m, Ar–H), 7.66–7.84 (10 H, m, Ar–H), 8.17 (1 H, dd, J = 8.3, 3.6 Hz, Ar–H). $^{13}C\{^1H\}$ NMR (126 MHz, CD_2Cl_2, 298 K) δ_C 55.1 (dd, J_{CP} = 74.8, 27.3 Hz, Ir–C–P), 117.7–118.1 (m, $[BAr^F_4]$ Ar–C), 121.7–128.3 (m), 128.3–130.6 (m), 131.6–131.7 (m), 132.5–134.4 (m), 134.7 (s), 135.1 (s), 135.2 (s), 135.3 (s, $[BAr^F_4]$ Ar–C), 136.2 (s), 137.2 (s), 142.5 (dd, J = 49.6, 8.6 Hz), 144.6–145.3 (m), 146.5–147.7 (m), 151.2 (d, J = 28.3 Hz), 153.6 (dt, J = 22.8, 2.7 Hz), 162.2 (q, $^1J_{CB}$ = 49.8 Hz, $[BAr^F_4]$ Ar–C). $^{31}P\{^1H\}$ NMR (202 MHz, CD_2Cl_2, 298 K) δ_P 3.0 (1 P, apparent dd, J_{PP} = 10.8, J_{PP} = 10.1 Hz, Ir–P), 10.4–11.0 (2 P, m), 36.9 (1 P, apparent dt, $^3J_{PP}$ = 25.9, $^3J_{PP}$ = 8.7 Hz, Ir–C–P). HRMS (ESI-TOF) *m*/*z*: $[M]^+$ calcd for $C_{73}H_{58}IrP_4$ 1251.3120; found 1251.3144. Elemental analysis: calc. for $C_{105}H_{70}BF_{24}IrP_4$: C, 59.6; H, 3.3; found: C, 59.3; H, 3.4%.

Preparation of complex 6

Method A: A solution of complex **2** (39.5 mg, 0.052 mmol) in DCM (5 mL) at −90 °C was treated dropwise with a solution of $Na[BAr^F_4]\cdot 2THF$ (53.4 mg, 0.052 mmol) in DCM (10 mL) and then 1,5-cyclooctadiene (7 μL, 0.057 mmol). The solution was allowed to come to room temperature and was stirred overnight. The reaction mixture was filtered and then the filtrate was evaporated fully. *n*-Hexane (5 mL) was added to the residue, triturated and then decanted. This process was repeated two additional times. The remaining residue was dissolved in DCM (1 mL), layered with *n*-hexane (10 mL) and then left to stand at room temperature. Colourless crystals of **6** formed from the solution were isolated by filtration and then dried under vacuum (70 mg, 79%).

Method B: A solution of compound **1** (5.5 mg, 0.01 mmol) in 1,2-dichloroethane (0.4 mL) was added dropwise to a solution of $[Ir(COD)_2][BAr^F_4]$ (12.7 mg, 0.01 mmol) in 1,2-dichloroethane (0.4 mL) at room temperature. The reaction solution was then heated to 95 °C for 18 h. $^{31}P\{^1H\}$ NMR spectroscopic analysis confirmed the formation of complex **6** in almost quantitative yield.

^1H NMR (500 MHz, CD_2Cl_2, 298 K) δ_H 1.15–1.26 (1 H, m, cyclooctadienylium), 1.55–1.68 (1 H, m, cyclooctadienylium), 1.68–1.80 (1 H, m, cyclooctadienylium), 1.80–1.91 (1 H, m, cyclooctadienylium), 2.53 (1 H, dt, J = 14.1, 8.8 Hz, cyclooctadienylium), 2.98–3.11 (1 H, m, cyclooctadienylium), 3.20–3.34 (1 H, m, cyclooctadienylium), 3.69–3.85 (2 H, m, cyclooctadienylium), 3.95 (1 H, t, J = 7.7 Hz, cyclooctadienylium), 4.59 (1 H, s, Ir–C–H), 4.92 (1 H, t, J = 7.9 Hz, cyclooctadienylium), 7.05–7.13 (6 H, m, Ar–H), 7.17–7.59 (26 H, m, Ar–H), 7.73 (8 H, s, $[BAr^F_4]$ Ar–H). $^{13}C\{^1H\}$ (126 MHz, CD_2Cl_2, 298 K) δ_C 20.5 (d, J = 3.8 Hz), 28.4 (d, J = 4.9 Hz), 31.8 (s), 40.5 (s), 49.9 (d, J = 15.5 Hz), 55.4 (d, J = 2.5 Hz), 69.1 (d, J = 32.6 Hz), 100.9 (s), 105.3 (s), 117.7–118.3 (m, $[BAr^F_4]$ Ar–C), 121.7–128.4 (m), 128.5 (s), 128.6–128.9 (m), 128.9–129.1 (m), 129.2–129.3 (m), 129.5 (s), 129.6–129.8 (m), 131.2 (d, J = 9.3 Hz), 131.7 (s), 131.8 (d, J = 11.0 Hz), 131.9 (s), 132.4 (d, J = 9.9 Hz), 134.5 (dd, J = 41.0, 10.6 Hz), 135.1 (s), 135.3 (s, $[BAr^F_4]$ Ar–C), 135.7 (d, J = 39.9 Hz), 137.1 (d, J = 6.7 Hz), 137.6 (d, J = 16.6 Hz), 157.6 (d, J = 29.7 Hz), 159.1 (d, J = 27.0 Hz), 162.3 (q, $^1J_{CB}$ = 49.8 Hz, $[BAr^F_4]$ Ar–C). $^{31}P\{^1H\}$ (202 MHz, CD_2Cl_2, 298 K) δ_P 9.1 (1 P, d, $^2J_{PP}$ 7.7 Hz, PCP pincer P), 17.5 (1 P, d, $^2J_{PP}$ = 7.7 Hz, PCP pincer P). HRMS (ESI-TOF) *m*/*z*: $[M]^+$ calcd for $C_{45}H_{40}IrP_2$ 835.2232; found 835.2232. calc. for $C_{77}H_{52}BF_{24}IrP_2$: C, 54.5; H, 3.1; found: C, 54.3; H, 3.4%.

Preparation of complexes 7a and 7b

Toluene (20 mL) was added to $[IrCl(COD)(PPh_3)]$ (119.6 mg, 0.20 mmol) and compound **1** (110.5 mg, 0.2 mmol) at room temperature and stirred overnight. The solution was then heated at 55 °C for two days. Afterwards, the solution was concentrated to approx. 5 mL and *n*-hexane (15 mL) was added to precipitate complexes **7a** and **7b**. The solids were filtered, washed with *n*-hexane (3 × 10 mL) and then dissolved in toluene (10 mL). The toluene solution was layered with *n*-hexane (20 mL) and left to stand at room temperature. Initially, colourless crystals of **7b** were isolated by fractional crystallization, filtration and then dried under vacuum. The filtrate was evaporated under vacuum, re-dissolved in toluene (5 mL) and then layered with *n*-hexane (15 mL) and left to stand at room temperature. Crystals of **7a** were isolated by filtration and then dried under vacuum (**7a**: 31 mg, 15%; **7b**: 105 mg, 50%).

7a: ^1H NMR (500 MHz, CD_2Cl_2, 298 K) δ_H −18.34 (1 H, td, $^2J_{HP}$ = 19.7, 13.8 Hz, Ir–H), 5.05 (1 H, d, $^4J_{HP}$ = 15.2 Hz, methine C–H), 6.72–6.87 (9 H, m, Ar–H), 6.90 (4 H, td, J = 8.2, 2.3 Hz, Ar–H), 7.00–7.46 (28 H, m, Ar–H), 7.70 (2 H, d, J = 7.7 Hz, Ar–H). $^{13}C\{^1H\}$ NMR (126 MHz, CD_2Cl_2, 298 K) δ_C 78.6–78.8 (m, methine C), 126.0 (t, J = 4.3 Hz), 127.3 (d, J = 10.0 Hz), 127.5 (t, J = 5.2 Hz), 127.8–128.1 (m), 129.4–129.6 (m), 129.7 (d, J = 6.7 Hz), 130.8 (d, J = 2.0 Hz), 134.4 (t, J = 5.4 Hz), 134.7 (s), 134.7–134.9 (m), 135.4 (t, J = 3.0 Hz), 136.1

(d, J = 10.8 Hz), 153.1 (t, J = 3.2 Hz). $^{31}P\{^1H\}$ NMR (202 MHz, CD_2Cl_2, 298 K) δ_P −6.1 (2 P, d, $^2J_{PP}$ = 11.4 Hz, POP pincer P′s), −1.2 (1 P, t, $^2J_{PP}$ = 11.4 Hz, PPh_3).

7b: ^1H NMR (500 MHz, C_6D_6, 298 K) δ_H −20.23 (1 H, td, $^2J_{HP}$ = 16.9, 9.3 Hz, Ir–H), 6.62–7.90 (44 H, m, Ar–H and O–H). $^{13}C\{^1H\}$ NMR (126 MHz, C_6D_6, 298 K) δ_C 84.7 (d, $^2J_{CP}$ = 82.5 Hz, C–OH), 126.5–126.8 (m), 126.8–127.1 (m), 127.4 (d, J = 9.1 Hz), 127.7 (t, J = 4.0 Hz), 128.6 (s), 129.4 (dd, J = 13.3, 8.8 Hz), 132.3 (t, J = 26.1 Hz), 133.5 (s), 133.9 (t, J = 5.3 Hz), 134.6 (t, J = 5.4 Hz), 134.9–135.7 (m), 136.1 (t, J = 27.1 Hz), 143.2 (d, J = 6.8 Hz), 165.5 (t, J = 14.1 Hz). $^{31}P\{^1H\}$ NMR (202 MHz, C_6D_6, 298 K) δ_P −2.1 (1 P, t, $^2J_{PP}$ = 12.7 Hz, PPh_3), 13.2 (2 P, d, $^2J_{PP}$ = 12.7 Hz, PCP pincer P′s). HRMS (ESI-TOF) m/z: $[M - Cl]^+$ calcd for $C_{55}H_{45}IrOP_3$ 1007.2311; found 1007.2294.

Conflicts of interest

The authors declare no competing financial interest.

Acknowledgements

We thank the National University of Singapore and the Singapore Ministry of Education for financial support (WBS R-143-000-586-112, R-143-000-697-114 and R-143-000-666-114).

Notes and references

1 (*a*) G. van Koten and D. Milstein, *Organometallic Pincer Chemistry, Topics in Organometallic Chemistry*, Springer, Berlin, 2013, vol. 40; (*b*) G. van Koten and R. A. Gossage, *The Privileged Pincer-Metal Platform: Coordination Chemistry & Applications*, Springer, 2015.

2 (*a*) D. V. Gutsulyak, W. E. Piers, J. Borau-Garcia and M. Parvez, *J. Am. Chem. Soc.*, 2013, **135**, 11776; (*b*) L. E. Doyle, W. E. Piers and J. Borau-Garcia, *J. Am. Chem. Soc.*, 2015, **137**, 2187; (*c*) L. E. Doyle, W. E. Piers, J. Borau-Garcia, M. J. Sgro and D. M. Spasyuk, *Chem. Sci.*, 2016, **7**, 921; (*d*) R. J. Burford, W. E. Piers and M. Parvez, *Organometallics*, 2012, **31**, 2949; (*e*) C. C. Comanescu and V. M. Iluc, *Chem. Commun.*, 2016, **52**, 9048; (*f*) C. C. Comanescu and V. M. Iluc, *Organometallics*, 2015, **34**, 4684; (*g*) C. C. Comanescu and V. M. Iluc, *Organometallics*, 2014, **33**, 6059.

3 Ir NHC PCP pincers are known, but their electronic structure differs greatly from $PC_{carbene}P$ pincers, as defined herein. See: A. F. Hill and C. M. A. McQueen, *Organometallics*, 2012, **31**, 8051.

4 (*a*) C. J. Moulton and B. L. Shaw, *J. Chem. Soc., Dalton Trans.*, 1976, 1020; (*b*) H. D. Empsall, E. M. Hyde, R. Markham, W. S. McDonald, M. C. Norton, B. L. Shaw and B. Weeks, *J. Chem. Soc., Chem. Commun.*, 1977, 589; (*c*) D. G. Gusev and A. J. Lough, *Organometallics*, 2002, **21**, 2601.

5 (*a*) W. Weng, S. Parkin and O. V. Ozerov, *Organometallics*, 2006, **25**, 5345; (*b*) R. J. Burford, W. E. Piers and M. Parvez, *Organometallics*, 2012, **31**, 2949.

6 (*a*) J. R. Logan, W. E. Piers, J. Borau-Garcia and D. Spasyuk, *Organometallics*, 2016, **35**, 1279; (*b*) J. D. Smith, J. R. Logan, L. E. Doyle, R. J. Burford, S. Sugawara, C. Ohnita, Y. Yamamoto, W. E. Piers, D. M. Spasyuk and J. Borau-Garcia, *Dalton Trans.*, 2016, **45**, 12669.

7 (*a*) R. J. Burford, W. E. Piers, D. H. Ess and M. Parvez, *J. Am. Chem. Soc.*, 2014, **136**, 3256; (*b*) A. V. Polukeev, R. Marcos, M. S. G. Ahlquist and O. F. Wendt, *Chem. Sci.*, 2015, **6**, 2060; (*c*) A. V. Polukeev and O. F. Wendt, *Organometallics*, 2017, **36**, 639; (*d*) A. V. Polukeev, R. Marcos, M. S. G. Ahlquist and O. F. Wendt, *Organometallics*, 2016, **35**, 2600; (*e*) M. S. Balakrishna, *Polyhedron*, 2017, DOI: 10.1016/j.poly.2017.07.026.

8 (*a*) S. Sung, T. Joachim, T. Krämer and R. D. Young, *Organometallics*, 2017, **36**, 3117; (*b*) S. Sung, J. K. Boon, J. J. C. Lee, N. A. Rajabi, S. A. Macgregor, T. Krämer and R. D. Young, *Organometallics*, 2017, **36**, 1609.

9 L. E. Doyle, W. E. Piers and D. W. Bi, *Dalton Trans.*, 2017, **46**, 4346.

10 Q. Teng and H. V. Huynh, *Dalton Trans.*, 2017, **46**, 614.

11 M. A. Bennett and D. L. Milner, *J. Chem. Soc., Chem. Commun.*, 1967, 581.

12 G. R. Clark, W. R. Roper and A. H. Wright, *J. Organomet. Chem.*, 1984, **273**, C17.

13 (*a*) K. Onitsuka, M. Nishii, Y. Matsushima and S. Takahashi, *Organometallics*, 2004, **23**, 5630; (*b*) L. M. Milner, L. M. Hall, N. E. Pridmore, M. K. Skeats, A. C. Whitwood, J. M. Lynam and J. M. Slattery, *Dalton Trans.*, 2016, **45**, 1717; (*c*) V. Cadierno, J. Díez, J. García-Álvarez and J. Gimeno, *Organometallics*, 2005, **24**, 2801; (*d*) R. P. Kamalesh Babu, R. McDonald and R. G. Cavell, *Organometallics*, 2000, **19**, 3462.

14 (*a*) R. H. Crabtree and C. P. Parnell, *Organometallics*, 1985, **4**, 519; (*b*) R. H. Crabtree, C. P. Parnell and R. J. Uriarte, *Organometallics*, 1987, **6**, 696; (*c*) R. H. Crabtree, R. P. Dion, D. J. Gibboni, D. V. McCrath and E. M. Holt, *J. Am. Chem. Soc.*, 1986, **108**, 7222.

15 (*a*) I. Zumeta, C. Mendicute-Fierro, A. Rodríguez-Diéguez, J. M. Seco and M. A. Garralda, *Organometallics*, 2015, **34**, 348; (*b*) D. L. Thorn, *Organometallics*, 1982, **1**, 197; (*c*) D. L. Thorn and J. C. Calabrese, *J. Organomet. Chem.*, 1984, **272**, 283.

16 J. Peone Jr. and L. Vaska, *Angew. Chem., Int. Ed. Engl.*, 1971, **10**, 511.

17 J. D. Smith, J. Borau-Garcia, W. E. Piers and D. Spasyuk, *Can. J. Chem.*, 2016, **94**, 293.

18 J. Arras, H. Speth, H. A. Mayer and L. Wesemann, *Organometallics*, 2015, **34**, 3629.

19 R. Dallanegra, A. B. Chaplin and A. S. Weller, *Organometallics*, 2012, **31**, 2720.

20 K. J. Jonasson, A. V. Polukeev, R. Marcos, M. S. G. Ahlquist and O. F. Wendt, *Angew. Chem., Int. Ed.*, 2015, **54**, 9372.